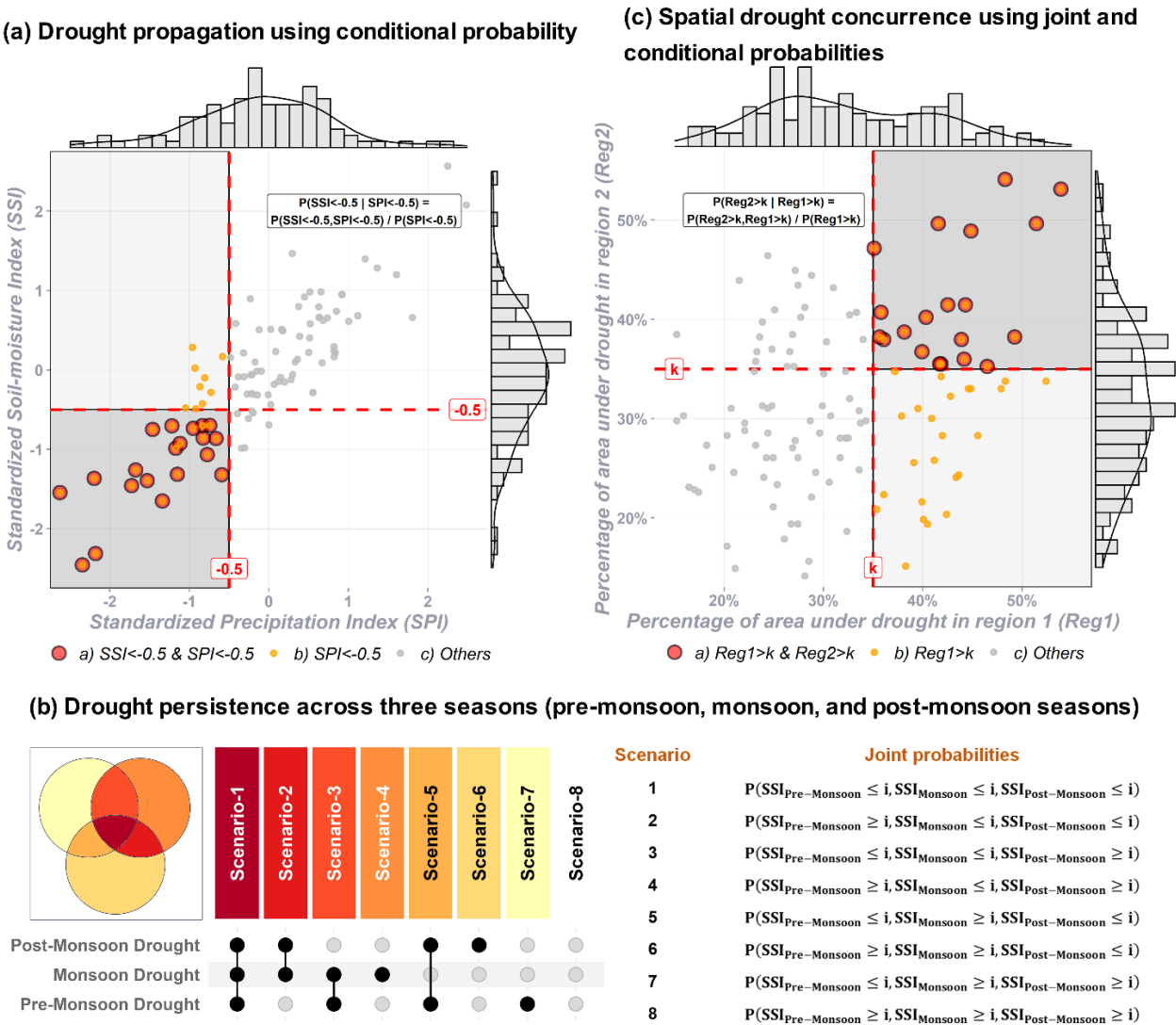# Probabilistic Analysis of Future Drought Propagation, Persistence, and Spatial Concurrence in Monsoon-Dominant Asian Region under Climate Change

5   Dineshkumar Muthuvel[1], Xiaosheng Qin[1*]

[1] School of Civil and Environmental Engineering, Nanyang Technological University,
50 Nanyang Ave, Singapore 639798

Correspondence to: Xiaosheng Qin (xsqin@ntu.edu.sg)

Abstract. This study examines future drought propagation (the temporal transition from meteorological to agricultural
10   droughts), persistence (inter-seasonal droughts), and spatial concurrence (simultaneous occurrence of monsoonal droughts across regions) under climate change using a multivariate copula approach in Monsoon-dominant Asia. Under the worst-case emission scenario (SSP5-8.5), South Asia (excluding Western and Peninsula India) and Eastern China are projected to experience intensified drought propagation compared to the historical period (1975-2014). In addition to increased propagation in these regions, the propagated agricultural droughts are expected to persist across seasons in the future. In terms of the return
15   period, all-season droughts that historically occurred once in more than 50 years could happen as frequently as every five years by the far-future (2061-2100) at the hydrologically significant Tibetan Plateau. Random Forest models indicate that the temperature is a key driver of future agricultural droughts in nearly half of the study area. The spatial concurrence of monsoonal agricultural droughts between region pairs such as South Asia (SAS), East Asia (EAS), Southeast Asia (SEA), and Tibetan region (TIB) was also assessed. Based on bivariate return periods of spatial concurrence, frequent future spatial drought
20   concurrence is anticipated between populous SAS and EAS compared to the historical timeframe, posing risks to water and food security. Conversely, SEA is projected to experience reduced spatial drought concurrence with other regions, which could encourage greater regional cooperation. Overall, this comprehensive approach which integrates three aspects of drought dynamics, offers valuable insights for climate change mitigation, planning, and adaptation.

(a) Drought propagation using conditional probability

(c) Spatial drought concurrence using joint and conditional probabilities

a) SSI<-0.5 & SPI<-0.5   b) SPI<-0.5   c) Others

a) Reg1>k & Reg2>k   b) Reg1>k   c) Others

(b) Drought persistence across three seasons (pre-monsoon, monsoon, and post-monsoon seasons)

Scenario	Joint probabilities
1	$P(SSI_{Pre-Monsoon} \leq i, SSI_{Monsoon} \leq i, SSI_{Post-Monsoon} \leq i)$
2	$P(SSI_{Pre-Monsoon} \geq i, SSI_{Monsoon} \leq i, SSI_{Post-Monsoon} \leq i)$
3	$P(SSI_{Pre-Monsoon} \leq i, SSI_{Monsoon} \leq i, SSI_{Post-Monsoon} \geq i)$
4	$P(SSI_{Pre-Monsoon} \geq i, SSI_{Monsoon} \leq i, SSI_{Post-Monsoon} \geq i)$
5	$P(SSI_{Pre-Monsoon} \leq i, SSI_{Monsoon} \geq i, SSI_{Post-Monsoon} \leq i)$
6	$P(SSI_{Pre-Monsoon} \geq i, SSI_{Monsoon} \geq i, SSI_{Post-Monsoon} \leq i)$
7	$P(SSI_{Pre-Monsoon} \leq i, SSI_{Monsoon} \geq i, SSI_{Post-Monsoon} \geq i)$
8	$P(SSI_{Pre-Monsoon} \geq i, SSI_{Monsoon} \geq i, SSI_{Post-Monsoon} \geq i)$

1 Introduction

Droughts, though not instantaneous, rank among the costliest disasters due to their prolonged and widespread impacts (Hao et al., 2016). They are known to manifest in different forms, beginning with meteorological drought caused by a precipitation deficit. If sustained, this can reduce runoff and soil moisture, leading to hydrological and agricultural droughts that impact entire ecosystems (Das et al., 2022). The propagation process is driven by multiple factors such as regional climate, teleconnections, topography, and anthropogenic activities (Han et al., 2019). Despite its complexity, understanding the progression of meteorological droughts into other forms is crucial for enhancing disaster preparedness and mitigation, particularly in the context of climate change. When a meteorological drought evolves into an agricultural or hydrological

drought, the risks are further heightened if the agricultural drought persists across multiple seasons (Ford and Labosier, 2014).
Given the spatial-temporal nature of droughts, such events can also occur simultaneously across multiple regions (Gaupp et
35   al., 2017). Therefore, a comprehensive assessment requires examining the characteristics of drought propagation, persistence,
and spatial concurrence.

The different drought forms are related to the components and processes of the hydrological cycle. The propagation
of different forms includes a certain time lag, which most studies focus on (Barker et al., 2016; Bevacqua et al., 2021; Wang
et al., 2024). Such studies use the cross-correlation between time series of monthly soil moisture (or streamflow) and
40   accumulated precipitation to deduce propagation time. While comparing propagation between basins of different climate
zones, Zhang et al. (2021) found arid basin to have lower propagation durations compared to humid and sub-humid basins.
Seasonality also influences propagation, and Dai et al. (2022) determined faster propagation in summer and autumn compared
to spring and winter. Apart from climatic factors, region specific characteristics of soil texture, vegetation, and topography
affect evapotranspiration and eventually the propagation duration (Wu and Hu, 2024). Hence, propagation duration estimated
45   using the correlation-based approach captures the interplay between the key factors. Further, propagation probability
measuring the likelihood of meteorological drought evolving to other forms are computed using copula functions (Xu et al.,
2021). Once a meteorological drought propagates to an agricultural drought, its persistence across seasons in a year could be
detrimental to satisfying domestic and agricultural water demands (Ford and Labosier, 2014). Inter-seasonal drought dynamics
can also be analysed using a copula-based multivariate approach, treating drought index values from each season as random
50   variables (Chen et al., 2016; Fang et al., 2019; Xiao et al., 2017). Beyond temporal aspects, the spatial concurrence (or
compounding) of droughts poses a significant threat to food or energy security when events occur simultaneously across
multiple breadbaskets or hydropower basins (Lv et al., 2025, 2024). In this context, studies have utilized copulas to estimate
the multivariate joint probability of key crop and pasture regions experiencing concurrent droughts (Gaupp et al., 2020; Sarhadi
et al., 2018).

55   Despite the extensive research on drought-related topics, several gaps remain to be addressed. First, various aspects
of droughts such as propagation, persistence, and spatial concurrence have largely been studied in isolation. Given the
spatiotemporal nature of droughts, it is crucial to examine these three aspects together for a more comprehensive assessment.
Secondly, recent review articles on drought propagation (Zhang et al., 2022; Zhou et al., 2024) highlight sufficient research
on the progression from meteorological to hydrological droughts (Sadhwani and Eldho, 2024; Zhou et al., 2023), but there is
60   a noticeable lack of studies on the transition from meteorological to agricultural droughts. Given the significant impact of
droughts on agriculture, these reviews emphasize the need for such studies. Finally, there are only a few regional studies on
the propagation of meteorological to agricultural droughts under climate change using future climate model data. These studies
often overlook the aspects of persistence and spatial concurrence.

To address the aforementioned gaps, this study proposes a comprehensive copula-based multivariate probabilistic
65   approach, utilizing climate model projection data. The approach is applied to the monsoon-dominant Asian region under
climate change, comparing drought characteristics between future and historical timeframes. Initially, the propagation

probability from meteorological to agricultural droughts is estimated for different seasons, and the influencing factors are identified. Next, the persistence of agricultural droughts across seasons is evaluated. Finally, the spatial concurrence of monsoonal agricultural droughts across various regions is assessed. This study offers a novel attempt to integrate these three aspects of droughts and analyse their interrelationships using multivariate copula functions. The resulting framework will identify key regions and patterns of future droughts, providing valuable insights for mitigation strategies.

2 Methodology

2.1 Drought propagation

2.1.1 Drought propagation duration

Indices such as Standardized Precipitation Index (SPI) and the Standardized Soil Moisture Index (SSI) are standard normal variates commonly used to quantify meteorological and agricultural droughts, respectively (Hao and AghaKouchak, 2013). SPI is based on monthly precipitation, while SSI relies on monthly soil moisture. These standardized indices are widely applied in drought studies due to their flexibility in capturing seasonal variations through different timescales (TS). Timescales represent accumulation periods, defined by aggregating input precipitation or soil moisture data over a specified number of months. The Pearson correlation between monthly SSI (for a timescale of one month) and SPI across various timescales (TS = 1 to 12) is calculated for each month. The timescale of SPI that shows the highest correlation with SSI indicates the drought propagation duration for the given month (Barker et al., 2016).

2.1.2 Drought propagation probability

The propagation of meteorological to agricultural drought, as shown in Fig. 1a, is assessed by the probability of agricultural drought occurrence (SSI ≤ -0.5) given the presence of pre-existing accumulated meteorological droughts over the propagation duration ($SPI_{TS} \leq -0.5$) (Long et al., 2024; Xu et al., 2021):

$$P(\text{SSI} \leq -0.5 \mid \text{SPI}_{TS} \leq -0.5) = \frac{C(G(-0.5),\ F(-0.5))}{F(-0.5)} \tag{1}$$

where G and F represent the marginal distributions of the random variables SSI and SPI (for the chosen timescale), respectively, while C denotes the bivariate copula function fitted to model the dependence between the two variables. The optimal copula function is selected from Clayton, Frank, Gaussian, Gumbel, Joe, Student t, BB1, BB6, BB7, and BB8 families based on maximum log-likelihood criterion (Xu et al., 2023). The drought propagation duration and conditional probability (Eq. 1) used to define propagation are computed for each grid and for every month across the study area.

2.1.3 Factors influencing propagation using Random Forest (RF) models

Random Forest (RF) models have recently been employed to identify the primary drivers of drought propagation (Dai et al., 2022; Li et al., 2023). These studies make use of interpretable outputs, such as the variable importance feature, to rank

the influential factors. Since meteorological droughts contribute to antecedent soil-moisture (SM) deficits, precipitation (Pr) is one of the key factors included in the RF model. Another important climatic factor is evapotranspiration, which, in turn, is influenced by temperature (T), humidity (H), vegetation cover (VC), solar radiation (SR), and wind (W) (Guo et al., 2017). These climatic variables serve as predictors, with soil moisture as the predictand in the RF models (f) (Breiman, 2001):

100    $SM \sim f(T + Pr + H + VC + SR + W + TS)$ (2)

To account for the memory effect of soil moisture, the predictors are standardized using timescales (TS) ranging from 1 to 12 months as one of the predictor variables (Muthuvel et al., 2023). The RF models are trained and tested using an 80:20 random data split for each grid point in the study area. Their performance is evaluated based on the coefficient of determination (R^2) values, calculated from the predicted and observed values in the testing dataset.

2.2 Drought persistence

Using joint probabilities, eight different scenarios of inter-seasonal droughts can be measured, as shown in Fig. 1(b). The worst-case scenario is the persistent all-season droughts. To this end, agricultural drought indices during the end months of Pre-Monsoon, Monsoon, and Post-Monsoon seasons are used as random variables. For regions above the equator, SSI values during May, September, and December are considered to represent the three respective seasons (Muetzelfeldt et al., 2021; Zhou et al., 2011). For regions in the equator and below the equator in SEA, the months of Sep, Jan, and May are used to study the inter-seasonal relationship since some of the grids receive rainfall during both Summer and Winter Monsoons (Van Noordwijk et al., 2017; Singh and Qin, 2020). Fang et al. (2019) used bivariate joint distributions considering indices during wet and dry seasons. Extending it to three seasonal drought variables, the probability of persistent agricultural droughts (defined by SSI) during the pre-monsoon, monsoon, and post-monsoon months in a given water year are estimated as:

115    $P(SSI_{Pre-Monsoon} \leq i, SSI_{Monsoon} \leq i, SSI_{Post-Monsoon} \leq i) = C(F(i), G(i), H(i))$ (3)

where F, G, and H are the marginal distributions of the three seasonal SSI values, while i refers to the drought severity thresholds. Shah and Mishra (2020) suggested using Gaussian copula for multivariate analysis involving more than two drought index values. Hence, the present study uses Gaussian copula (C) to represent the dependence among the three random variables of seasonal droughts. In terms of return periods ($T_{Persistent\ Droughts}$), drought persistence for a given severity threshold (i) is derived as (Fang et al., 2019):

120    $T_{Persistent\ Droughts} = 1 / P(SSI_{Pre-Monsoon} \leq i, SSI_{Monsoon} \leq i, SSI_{Post-Monsoon} \leq i)$ (4)

Apart from the worst-case scenario of persistent all-season droughts, there are other scenarios, such as two-season droughts (only two of the three seasons are drought-affected in a water year), isolated single-season droughts (only one of the three seasons is drought-affected in a water year), and no-drought (all three seasons in a water year have above normal SSI) scenarios. All eight scenarios will be computed using Gaussian copula (C) based on trivariate probabilities (similar to Eq. 3) described in Table S1.

2.3 Spatial concurrence

One of the most commonly used drought attributes is the spatial coverage of drought, measured as the percentage of grids experiencing drought (SSI < i) within a given region during a specific month. Following the approach by Yu et al. (2023), which uses copula-based conditional probability to analyse spatial concurrence, if Reg_2 and Reg_1 represent the spatial agricultural drought coverages (SSI < i) of two regions, the drought concurrence between them is defined as:

$$P(Reg_2 \geq k \mid Reg_1 \geq k) = \frac{1-F(k)-G(k)+C(F(k),G(k))}{1-F(k)} \tag{5}$$

where k is the threshold of spatial drought coverage, and F and G are the marginal distributions of Reg_1 and Reg_2 respectively. The bivariate return period to estimate monsoonal concurrent droughts (T_{CD}) are derived as (Muthuvel and Mahesha, 2021b):

$$T_{CD} = 1/P(Reg_2 \geq k, Reg_1 \geq k) = 1/(1 - F(k) - G(k) + C(F(k), G(k))) \tag{6}$$

After fitting appropriate bivariate copula C (Similar to Eq. 1), conditional probability curves (Eq. 5) and return period contours (Eq. 6) for various drought coverage thresholds (k) will be plotted. Figure 1c shows the joint (upper right shaded domain) and conditional (upper right and right shaded domains) probability domains between the two regions exceeding the drought coverage threshold (k) used to derive Eq. (5) and (6). While empirical marginal distributions are used in Eq. (1) to (4), appropriate theoretical marginal distributions, selected from Generalized Extreme Value, Gamma, Gumbel, Lognormal, and Pearson Type III distributions based on the lowest Akaike information criterion (AIC) values, are fitted in Eq. (5) and (6) to produce smooth drought frequency curves (Datta and Reddy, 2023). The entire analysis is conducted in the R programming language (v4.3.3; R Core Team 2024), utilizing packages such as lmomco (Asquith, 2024) for marginal distribution fitting, rvinecopulib (Nagler and Vatter, 2023) for copula functions, rnaturalearth (Massicotte and South, 2023) for mapping, and ggplot2 (Wickham, 2016) for figure plotting.
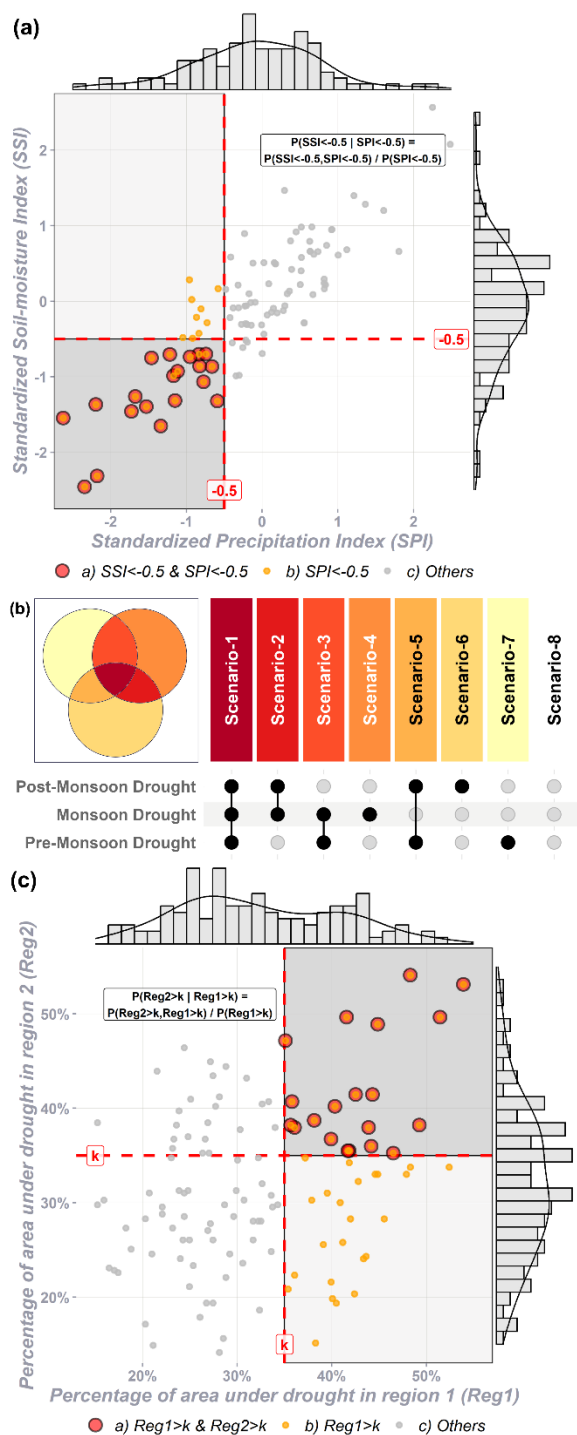
Figure 1: (a) Domain of conditional probability defining the propagation from meteorological to agricultural drought, (b) Venn diagram of all possible inter-seasonal drought scenarios, and (c) domain of conditional and joint exceedance probability for studying drought spatial concurrence.

3 Study Area and Data

The study area of monsoon-dominant Asia (Fig. 2a and Fig. 2b) comprises countries in the domain of Tibet (TIB), South Asia (SAS), East Asia (EAS), and Southeast Asia (SEA). The grid points at 1º x 1º spatial resolution within the administrative boundaries of 21 countries are used in the study. The observed monthly precipitation and soil moisture data between 1975 and 2014 from GLDAS (Global Land Data Assimilation System, version 2.0) are used for reference (Rodell et al., 2004). The study uses the worst-case emission scenario of SSP5-8.5 (Shared Socioeconomic Pathway) from Coupled Model Intercomparison Project phase 6 (CMIP6) for future projections. Multi-Model Ensembles (MMEs) of monthly precipitation (pr) and soil moisture (mrso) are calculated using Bayesian Model Averaging (BMA) based on simulated historical climate and observed data using R library BMA (Raftery et al., 2024). While MMEs using simple averages with equal weights for all models have proven effective in studying droughts (Feng et al., 2023), the potential over- or underestimation of variables by individual models can be mitigated by assigning appropriate weights through BMA (Zhai et al., 2020; Muthuvel et al., 2023). A detailed explanation of the MMEs based on the Bayesian averaging method is provided in Tian et al. (2025). A comparison of the spatial monthly distributions between the MMEs and observed data reveals substantial similarity for both rainfall (Fig. 2c) and soil moisture (Fig. S1 in the Supplementary Materials). Additionally, the MME outperforms the eight individual models (BCC-CSM2-MR, CanESM5, CNRM-CM6-1, CNRM-ESM2-1, GFDL-ESM4, IPSL-CM6A-LR, MIROC-ES2L, and MRI-ESM2-0) (Fig. S2 and Fig. S3 in the Supplementary Materials) and will therefore be used to compute the drought indices. The individual GCMs are interpolated and regridded to a uniform spatial resolution of 1º x 1º. These selected climate models also provide access to additional monthly variables, including temperature (tas), humidity (huss), vegetation cover (lai), radiation (rsds), and wind (sfcWind), which will be used in the RF models (Eq. 2). The climate models are freely available and managed by the World Climate Research Program (WCRP, 2024).
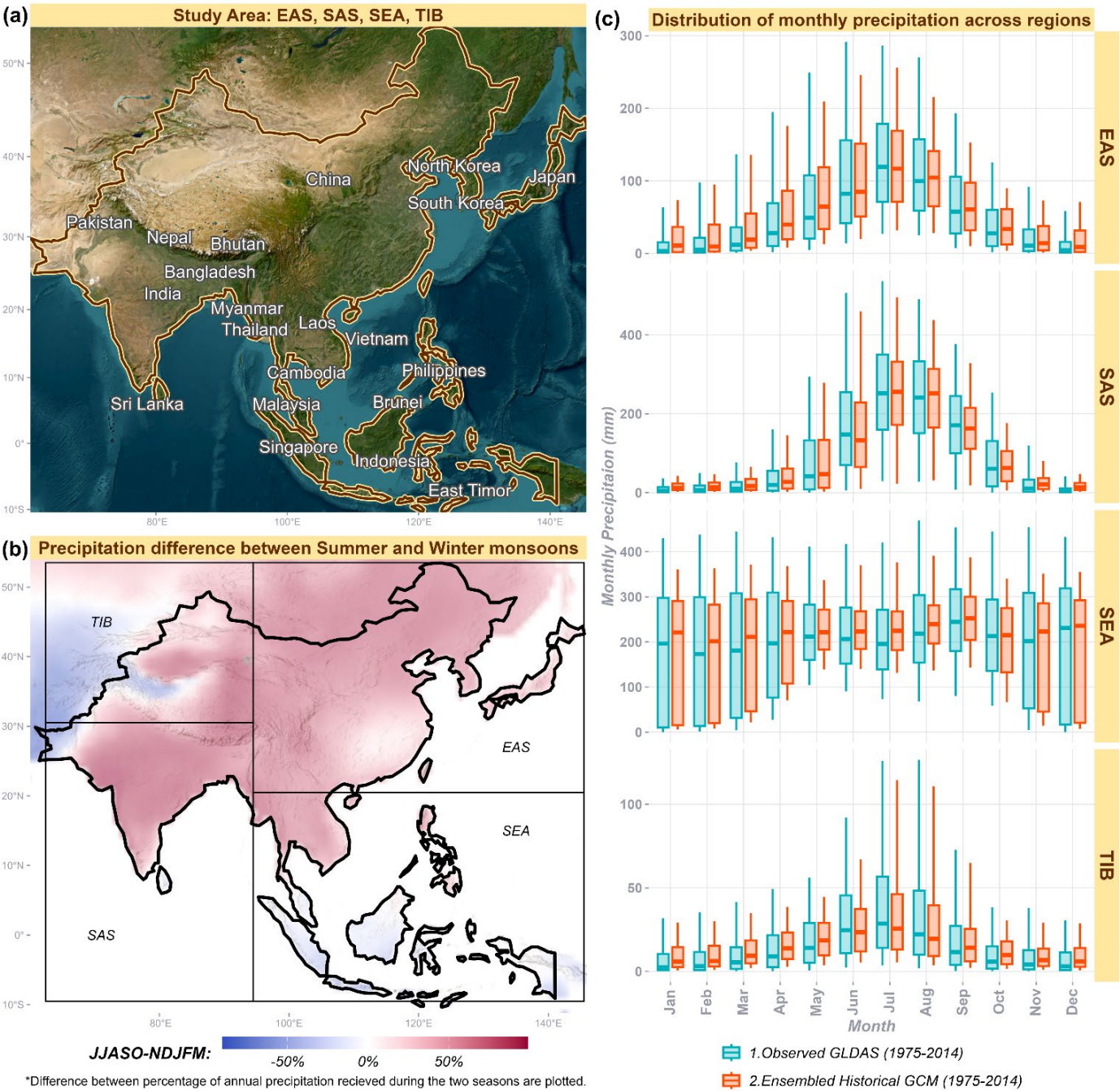
Figure 2: (a) Study area of monsoon-dominant Asia with its boundary, (b) percentage difference in precipitation between Summer (June-October) and Winter (November-March) monsoons, and (c) monthly comparison of observed and historical GCM precipitation data across four regions.

4 Results and discussion

4.1.1 Drought propagation duration

Initially, propagation durations based on the timescales of SPI (TS between 1 and 12) corresponding to the maximum correlation with monthly SSI (TS = 1) are estimated for each month across the entire study area, with their distributions presented in Fig. 3a. Unlike earlier studies (Guo et al., 2020) which considered all months together to estimate drought propagation duration, calculating propagation duration for each month is crucial in monsoon-dominant regions with pronounced seasonal rainfall disparities. During the historical period, approximately 32% of the study area exhibited propagation durations of three months or less in June. The percentage of the area experiencing such short-term rapid propagation durations (TS = 1 to 3) steadily increase to 55% by October before progressively declining to 23% by April. Conversely, the percentage of the area with prolonged propagation duration (TS > 6 months) increases steadily from 25% in October to 55% in May, followed by sharp decline during the monsoon months (June to October). This patten aligns with the seasonal variability associated with the onset and withdrawal of the monsoon in the region. Soil moisture replenishes with the onset of the monsoon, as indicated by shorter timescales from June to October. Most areas in the study region receive substantial precipitation during this period, and soil moisture is heavily dependent on it.

Owing to the sensitivity of soil-moisture to monsoon precipitations, prolonged propagation durations are observed in the post-monsoon months. Notably, parts of arid SAS and TIB exhibit propagation durations up to 12 months during May in the historical timeframe, as shown in Fig. 3b. From the maps of propagation durations (Fig. S4 in Supplementary Materials), regions in SEA regions, such as Indonesia and the Malay Peninsula, show comparatively shorter propagation durations despite differences in seasonality. Unlike the temporal skewness of rainfall distribution during the monsoon in the study area, rainfall in these regions is more evenly distributed across most months of the water year. The percentage distribution of propagation durations in the near (2021-2060) and far future (2061-2100) remains largely similar to that of the historical timeframe (1975-2014), aligning with the monsoon progression. Similar findings of minimal shifts in propagation durations under climate change have been reported in studies from South China (Zhou et al., 2023, 2021), albeit for propagation from meteorological to hydrological droughts.
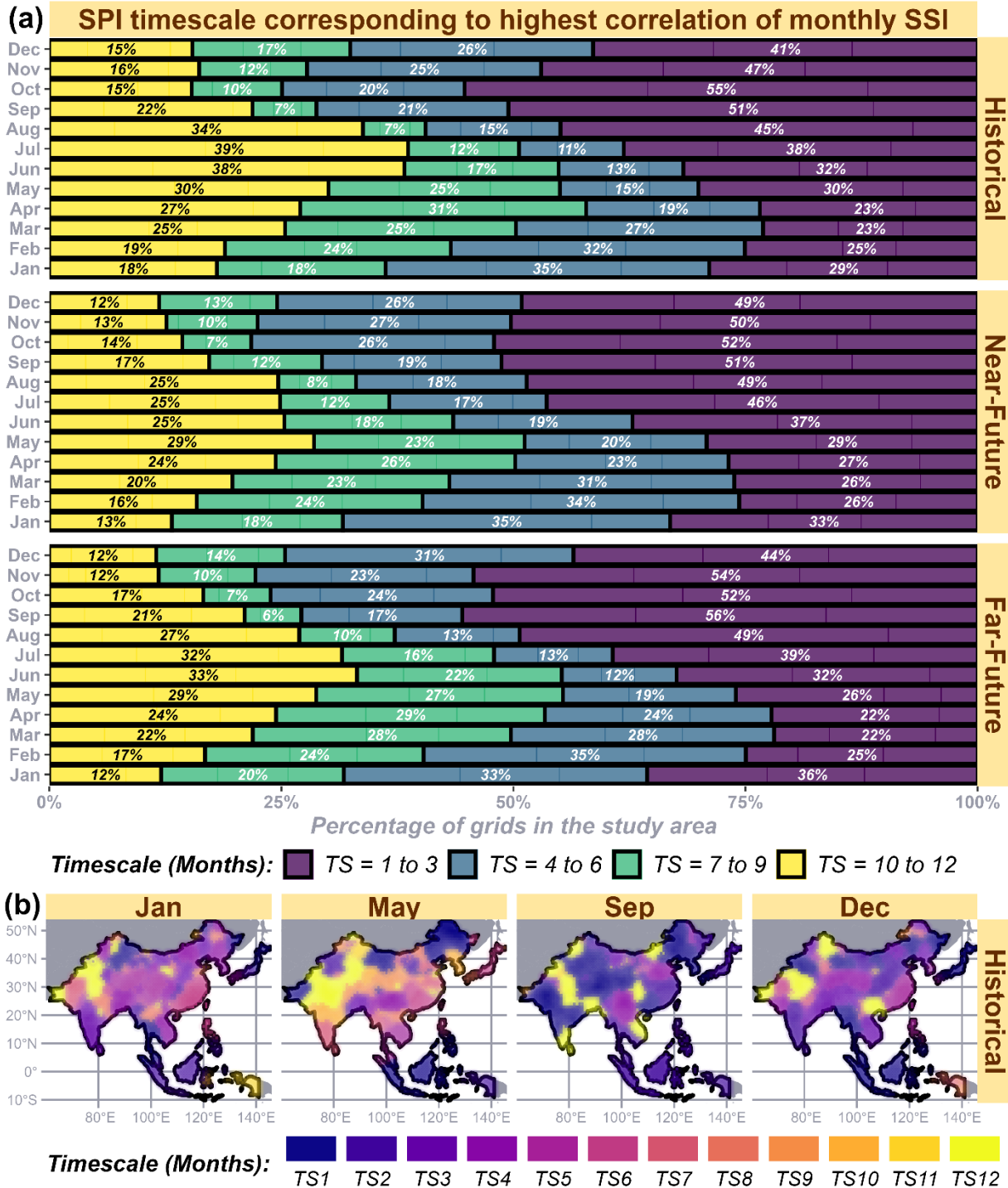
Figure 3: Propagation durations (in timescale, TS) shown as (a) percentages across the study area for each month in different timeframes and (b) spatial maps for different seasons in the historical timeframe.

4.1.2 Drought propagation probability

205   Conditional probabilities (CP), which defines the propagation of agricultural drought from meteorological droughts for each month, are calculated based on the previously computed propagation durations (SPI timescales, Fig. 4). Comparing the median CP values, half of the grids in EAS exhibit propagation probabilities below 0.25 in the historical timeframe across all seasons (Fig. 4a). In the near- and far-future timeframes, the median CP values increase to approximately 0.41 and 0.52 across seasons, respectively. In SAS, the historical median CP reaches its highest value in September (0.33) at the end of the
210 monsoon season, followed by December (0.27), January (0.23), and May (0.2) towards the region's water year end. Similar to EAS, SAS shows higher median CP values in the near- and far-future timeframes compared to the historical period. However, unlike the historical timeframe, future propagation probabilities in SAS during non-monsoon months (median CPs of 0.58, 0.61, and 0.64 for December, January, and May, respectively, in the near future) exceed those of monsoon months (median CP of 0.44 for September in the near future). In SEA, the distribution of CP values remains largely consistent between the
215 historical and near-future timeframes across all seasons, indicating that drought propagation probabilities remain stable. However, in the far-future timeframe, median CP values drop significantly compared to the other two periods. For instance, the historical median CP of about 0.42 across all months declines sharply to 0.25, 0.34, 0.32, and 0.24 during January, May, September, and December, respectively, in the far future. The reduction in CP values is even more pronounced in TIB, where the historical median CP of approximately 0.50 decreases to 0.15 and 0.12 in the near- and far-future timeframes, respectively.
220 This decline suggests that meteorological droughts are less likely to evolve into agricultural droughts in the future compared to the historical period, which is a positive indication for grids in TIB and SEA. Despite minimal shifts in the propagation durations estimated earlier, significant changes in propagation probabilities are expected across the study area in the future.

      The difference in CP values during the near and far future compared to historical timeframes are spatially depicted in Fig. 4b. Regions with increased propagation probability in the far future across seasons, relative to the historical period, include
225 most of SAS (excluding Peninsular and Western India) and Eastern China, making these areas more vulnerable to meteorological droughts transitioning into agricultural droughts. These regions have also been identified as prone to compound dry hot events (the coexistence of meteorological droughts and above-normal hot events) under future climate change scenarios (Feng et al., 2025; Prabhakar et al., 2023). Rising temperatures associated with climate change are likely to exacerbate this risk by depleting soil moisture and accelerating the drought propagation process. In contrast, regions such as the arid Xinjiang
230 province in northwestern China (TIB domain) and Mainland Southeast Asia (except during May) are expected to experience reduced drought propagation in far-future compared to the historical timeframe. Previous studies (Try and Qin, 2024; Wang et al., 2022) project more frequent extreme precipitation events in these areas under the SSP5-8.5 scenario, which could mitigate drought propagation.
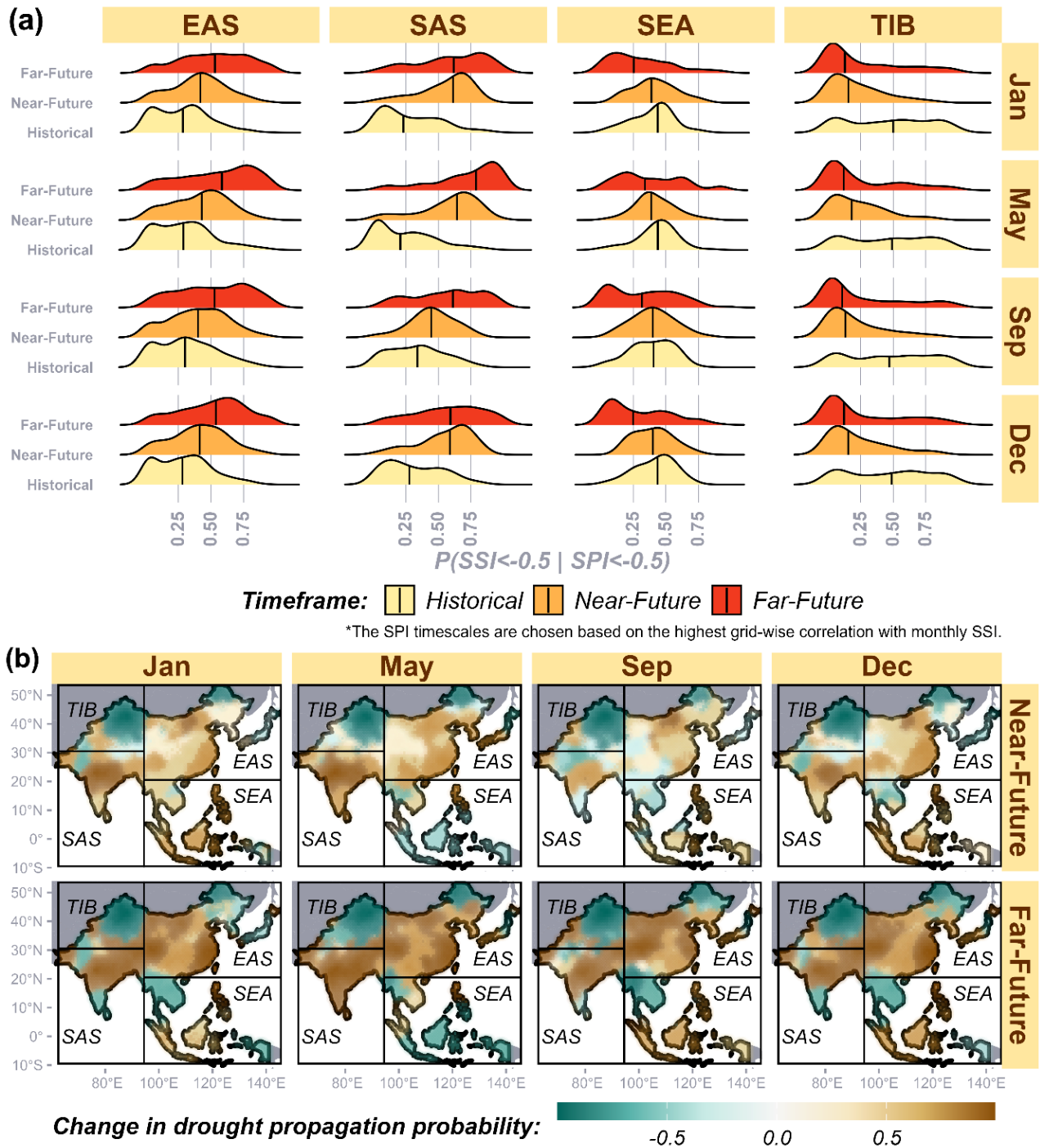
Figure 4: (a) Comparison of propagation probabilities across four regions, seasons, and timeframes, and (b) spatial maps showing the differences in propagation probabilities between future and historical timeframes.

4.1.3 Factors affecting propagation

Several climatic factors contribute to soil moisture depletion and exacerbate the drought propagation process. Key
240 drivers identified by previous studies (Wang et al., 2023) include precipitation, air temperature, specific humidity, solar
radiation, near-surface wind speed, and leaf area index (vegetation), all of which are used as predictors in RF models to estimate
soil moisture. To account for their lag effects on monthly SSI, standardized indices of these variables at timescales ranging
from 1 to 12 months are incorporated into the model. An RF model is developed for each grid, and its performances is evaluated
using the coefficient of determination (R^2). Overall, FR models perform better in the future timeframes, with most achieving
245 R^2 values above 0.75 in the far future and above 0.45 in the near future, compared to lower R^2 values in the historical period
(Fig. 5a). The distribution of variable importance in the historical timeframe reveals similar quantile values for temperature,
humidity, and radiation (Fig. 5b), although temperature tends to have higher quantiles. The predictor with the highest variable
importance is identified as the key driver. As shown in Fig. 5c, in the historical timeframe, humidity (32% of the study area)
and vegetation cover (25% of the study area) are the primary drivers of agricultural droughts. However, in future timeframes,
250 temperature emerges as the dominant driver in nearly half of the study area (see Fig. S5 in the Supplementary Materials). This
finding, highlighting the increasing influence of temperature on soil moisture deficit, aligns with the projected rise in compound
drought and heatwave events reported by Tripathy et al. (2023).
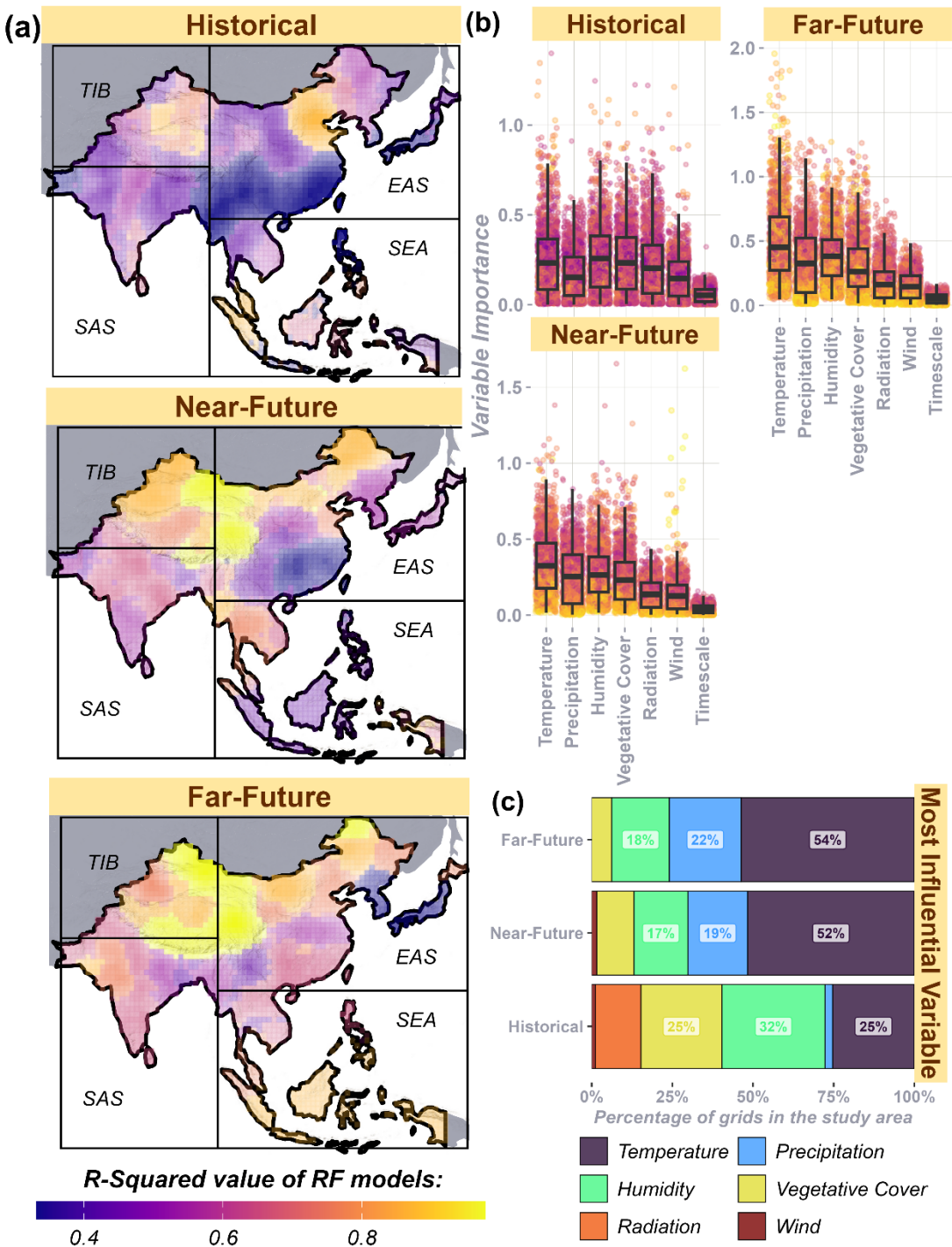
Figure 5: (a) Performance evaluation (R² values) of Random Forest (RF) models for each grid across timeframes, (b) variable importance values of predictors used in the RF models, and (c) most important variable (highest importance value in an RF model) in each timeframe across the study area.

4.2 All-season persistent droughts

Having identified regions sensitive to the propagation of meteorological to agricultural droughts, it is important to
also focus on the persistence of these agricultural droughts across seasons. The joint probability (JP) of agricultural droughts
(monthly SSI < 0) during the pre-monsoon, monsoon, and post-monsoon months in a given water year is used to define
persistence (Fig. 6a). Among the eight possible combinations of seasonal droughts, the probability of all-season droughts and
its complementary scenario of all wet seasons are higher than those isolated seasonal droughts. In the historical timeframe,
half of the study area has JP values more than 0.17 for all season droughts, which increases to about 0.25 in both the near- and
far-future timeframes. In contrast to the increase in all-season droughts, the median JP for all-season wetness decreases from
0.25 in the historical timeframe to 0.2 and 0.18 in the near and far-future, respectively. When plotting the difference in JP
values between the future timeframes and the historical timeframe, regions identified as at higher risk of all-season droughts
in the near future include central India (in SAS), regions in EAS, and the Philippines (Fig. 6b). The differences in JP values
are more pronounced in the far future, indicating an amplified risk of persistent all-season droughts. Liang et al. (2023) reported
that CMIP6 models predict an increase in both extreme and mean precipitation values in northwestern China (in the TIB
domain) in the future, compared to the historical values, while a decrease in precipitation is projected for the southwestern
region (in the EAS domain). The current results also reflect this pattern, with an increase (and decrease) in future JP values in
these regions, albeit from a drought perspective.

Regarding return periods of all-season persistent droughts (Fig. 7), northwestern China (in the TIB domain) exhibits
a return period of less than 2 years for SSI < 0 in the historical timeframe, which increases drastically to over 50 years in the
far future (Fig. 7a). When comparing across timeframes, severe persistent all-season droughts (SSI < -0.8 across seasons) are
historically rare, occurring only once in more than 50 years in approximately 80% of the study area (Fig. 7b). However, such
events are projected to become more frequent in the future. Specifically, only about 12% of the study area experiences frequent
severe persistent all-season droughts (return periods of less than 20 years) in the historical timeframe, but this increases to 23%
and 39% in the near- and far-future timeframes, respectively. These frequent severe events in the future are predominantly
concentrated in EAS grids. While severe persistent drought events (return periods greater than 50 years) remain rare in SAS
(except for central India) for SSI < -0.8, events with SSI < -0.5 could still occur frequently (return periods of less than 20
years) across the region. Consistent with the reduced propagation probability (as defined by CP) observed in mainland SEA in
the far future, persistent droughts in this region are rare, regardless of the SSI threshold.

(a)

(b)

Change in persistent all season drought probability:
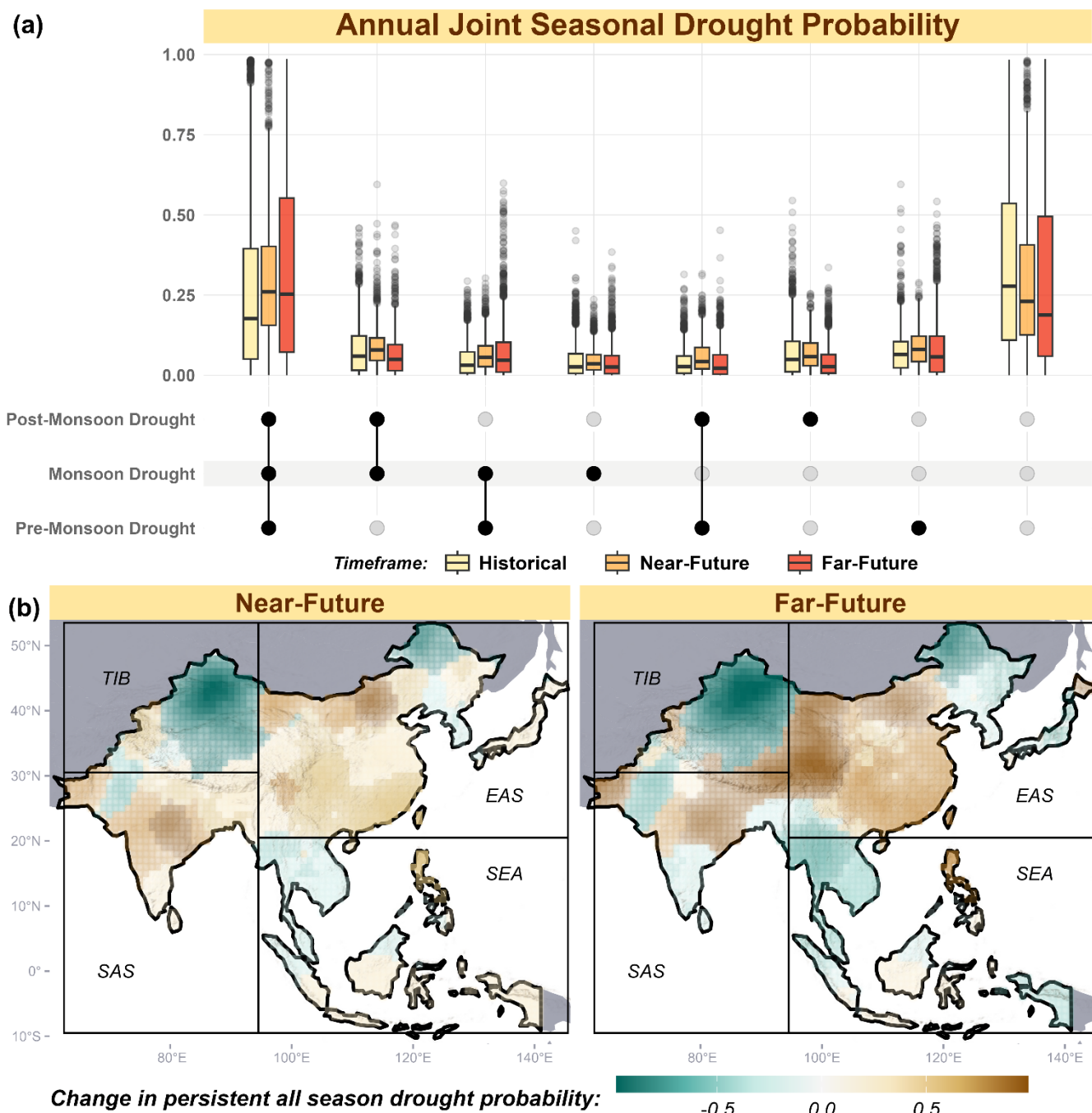
*The differences between joint probabilities of future and historical timeframes of all season droughts are shown.

Figure 6: (a) Joint probabilities of all inter-seasonal drought scenarios across the study area for three timeframes, and (b) maps showing differences in all-season drought probabilities between future and historical timeframes.
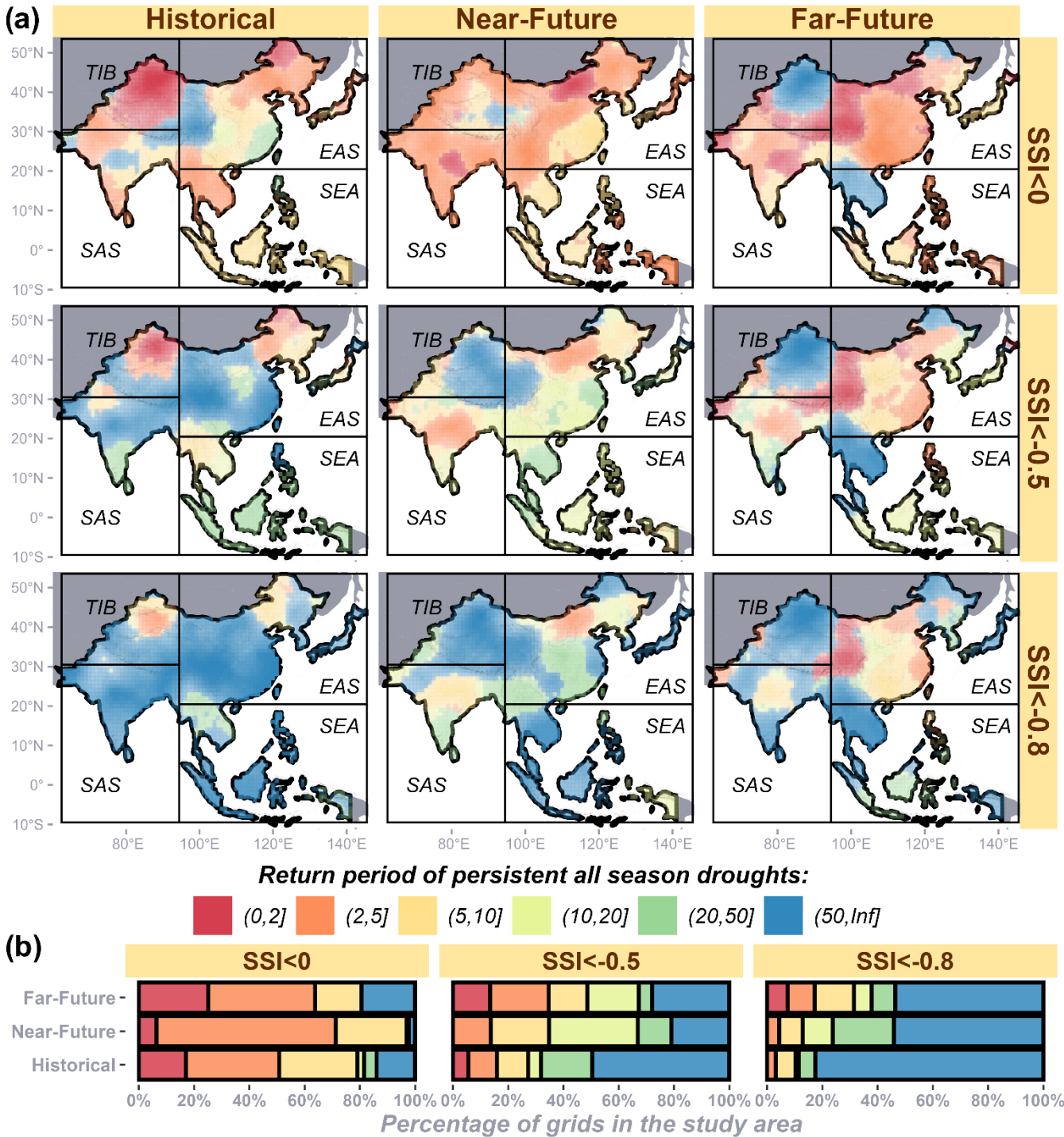
Figure 7: Return periods of persistent all-season droughts for various agricultural drought severity levels across timeframes, shown as (a) maps and (b) percentages of the study area.

4.3 Drought spatial concurrence

295   Considering the spatial disparities in the propagation and persistence of future droughts, the synchrony (or lack thereof) of monsoonal droughts across regions is examined to understand interconnected risks. The annual concurrence of drought between region pairs is assessed by examining the agricultural drought during monsoon months in each region. Figure 8 illustrates the probabilities of droughts exceeding a given spatial coverage threshold (k) in one region (Reg2) under the condition that the same spatial coverage threshold is exceeded in another region (Reg1). For instance, when 25% of EAS

300   (Reg1) is under drought, there is a 62% probability that 25% of SAS (Reg2) will also experience droughts in the historical timeframe. This probability increases to approximately 75% and 90% in the near- and far-future timeframes, respectively. Considering the dense populations and significant agricultural activity in these regions, the high spatial concurrence of future monsoonal droughts is concerning. In contrast, the conditional probability of drought concurrence between EAS (Reg1) and SEA (Reg2) decreases from 0.57 in the historical timeframe to 0.48 in the near future, and further to 0.27 in the far future. A

305   similar reduction is observed between SAS (Reg1) and SEA (Reg2). For TIB (Reg2), the conditional probability of droughts exceeding 25% spatial coverage in other regions (Reg1) remains similar between the historical and far-future timeframes but is significant lower in the near future.

    Overall, SAS and EAS are projected to experience an increase in simultaneous monsoonal droughts, while SEA shows reduced concurrence with the two regions (Fig. 9). The spatial concurrent joint return periods are estimated and compared

310   across timeframes using a historical reference event for these regions. For example, a drought event affecting 36% of EAS and 38% of SAS in a given year currently has a return period of approximately 30 years. However, such an event is expected to occur every 10 years in the near future and less than every 5 years in the far future, indicating more frequent spatially concurrent droughts between EAS and SAS. Large-scale widespread droughts affecting 50% of both EAS and SAS have return periods between 20 and 50 years in the future, which might not occur in the other timeframes. In contrast, the same historical reference

315   event, which currently has a return period of 10 to 20 years for EAS and SEA, is projected to occur only once every 50 years or more in the future timeframes, highlighting the reduced likelihood of spatially concurrent droughts involving the SEA region. Similar patterns of reduced likelihood of spatially concurrent droughts in the far future could happen between SAS and SEA. Specifically, widespread droughts become rare in SEA during far-future timeframes, such that droughts covering 40% of SEA could occur once in more than 50 years compared to more frequent events in other timeframes. Although most grids

320   in TIB are not agriculturally productive, several rivers in the other three regions originate in this region, and hence, analyzing spatial drought concurrence involving TIB has hydrological significance (Fig. S6). The historical reference event of simultaneous droughts covering 31% and 42% of TIB and EAS has a return period of about 10 years in the historical timeframe, which becomes rare in the near future (about 50 years return period). However, such events could once again become frequent with 2 to 5 years return period in the far future. This pattern of spatially concurrent widespread drought events becoming rare

325   in the near future but frequent in the far future is also noticed from the return period profile between TIB and SAS regions.

TIB-SEA has reduced future spatial concurrence similar to the return period profiles in the SEA-EAS and SEA-SAS region pairs.

Figure 8: Probability of a region exceeding different drought spatial coverage (k), conditioned on similar spatial coverage in another region, compared across timeframes.
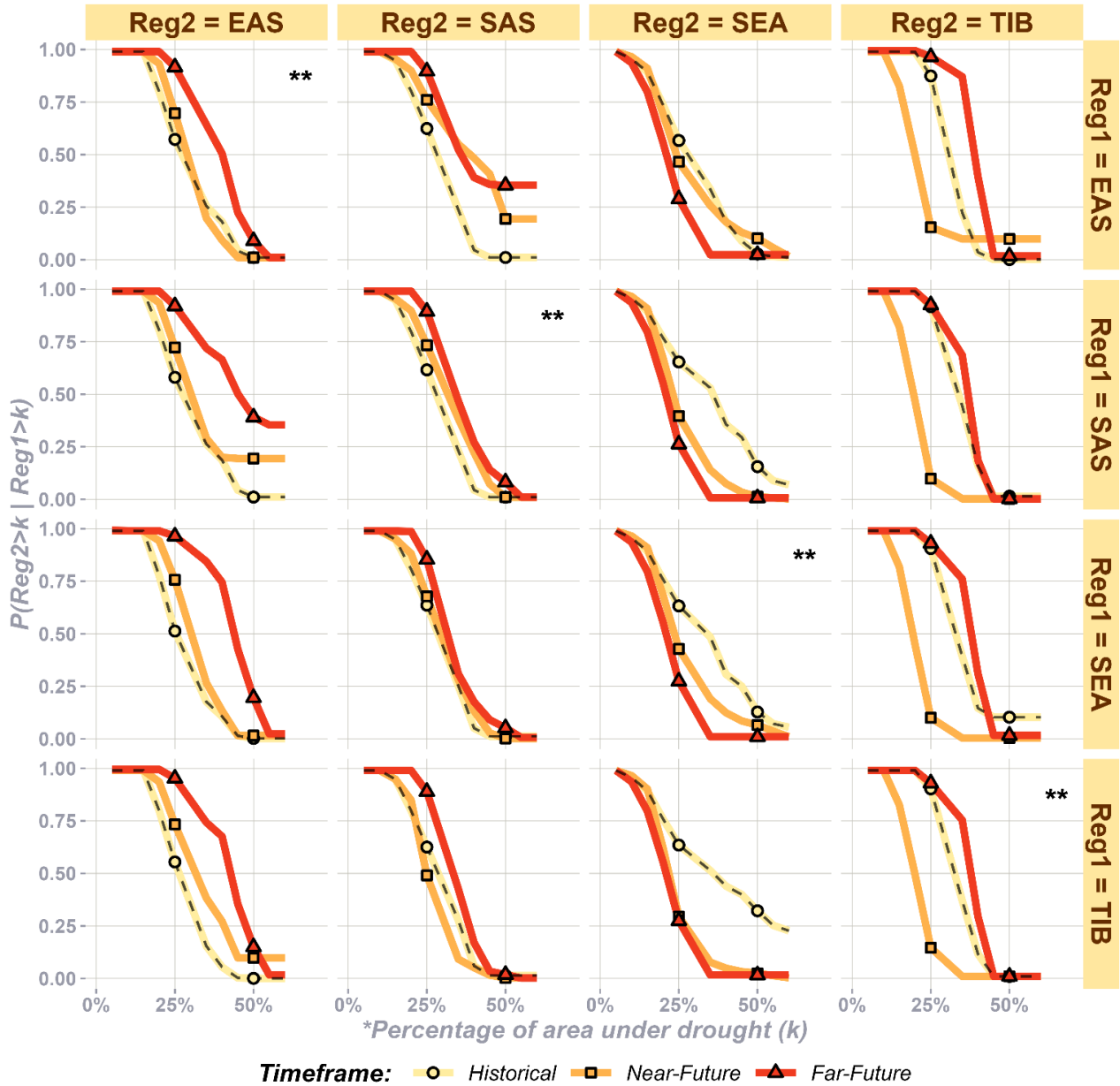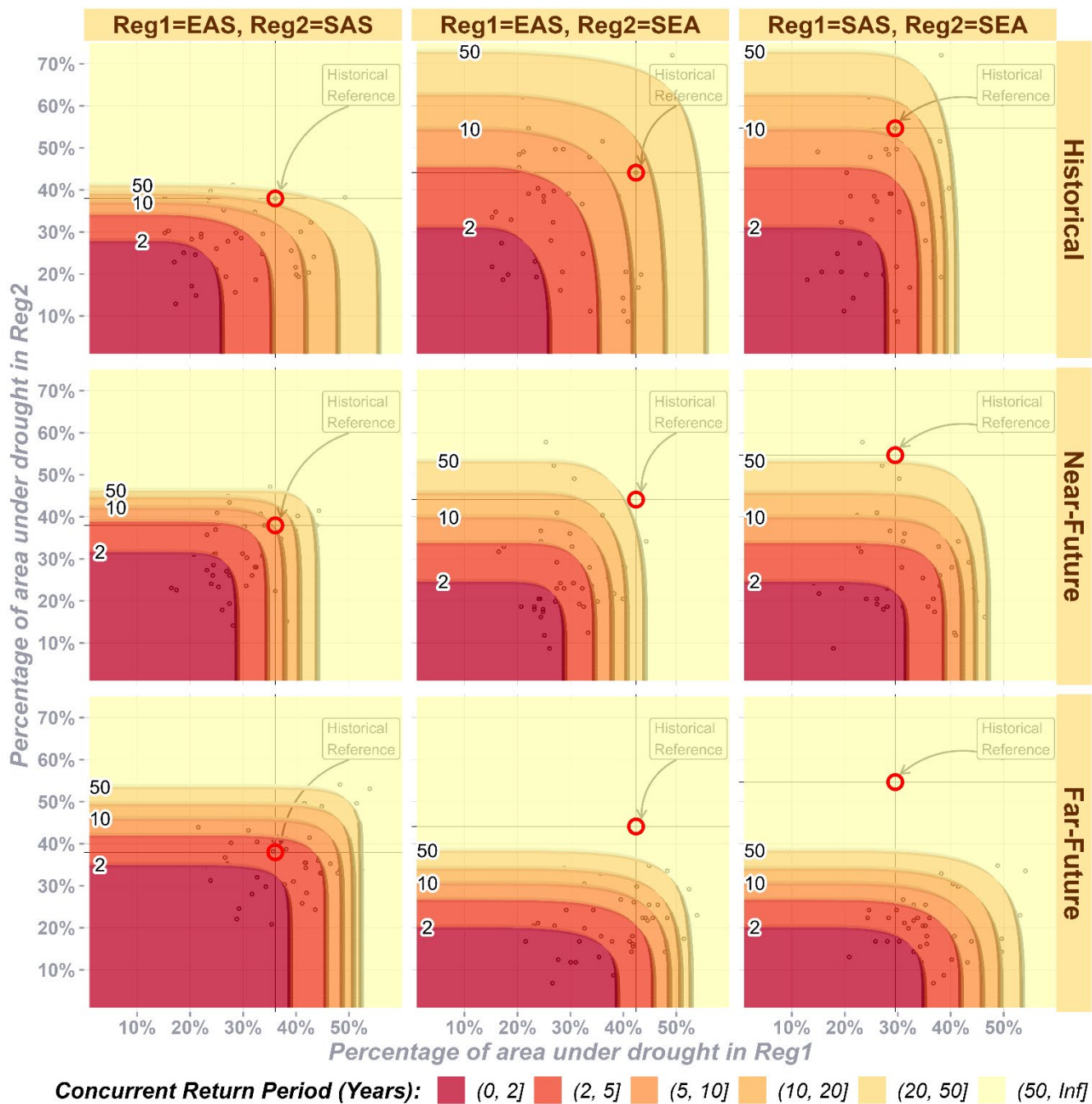
Figure 9: Spatial concurrent return periods between region pairs across timeframes, with random variables (percentage of area under drought annually) shown as black dots.

4.4 Further Discussion

While previous studies on drought propagations often focus on the transition of precursor meteorological droughts to agricultural or hydrological droughts, the persistence and spatial concurrence of the antecedent drought forms are often
340 overlooked. The current study, however, highlights a strong correlation between the propagation process (CP) and the persistence of agricultural droughts across seasons (JP) in the future (Fig. 10a). Differences between future timeframes and historical CP values were compared with corresponding JP values for all grids using scatterplots. The strong correlation (approximately 0.85, $p < 0.001$) indicates that grids experiencing accelerated propagation are also prone to persistent all-season droughts, and vice versa, in the future. In the far-future timeframe, a cluster of grids along the southeastern margin of the
345 Tibetan Plateau (90°E to 104°E and 28°N to 35°N) exhibits significantly higher propagation and persistence compared to the historical timeframe (Fig. 10b). This cluster, often referred to as the "Asian Water Tower" (Leng et al., 2023), is of hydrological significance, as it serves as the origin for major rivers such as Brahmaputra (Yarlung Tsangpo), Irrawaddy, and Salween. It also overlaps with the upper reaches of the Mekong, Yellow, and Yangtze rivers, which are critical for agriculture, industry, and livelihoods in both EAS and SAS regions. The strong negative correlation between soil moisture and temperature (Fig. S7
350 in Supplementary Materials) under future climate change scenarios contributes to the accelerated propagation and persistence of droughts in this region. These findings align with reports by Li et al. (2022) and Zhang et al. (2023), which document climate-change-induced terrestrial water deficits in Asia's Water Tower under the SSP5-8.5 scenario, further supporting the current results.

The projected increase in future spatial drought concurrence between EAS and SAS could have significant
355 implications, including synchronized crop failures (Mehrabi and Ramankutty, 2019; Muthuvel and Sivakumar, 2024a), challenges in transboundary water management (Williams, 2018), and energy-sharing difficulties (Lv et al., 2024). These risks are further exacerbated by the projected rise in the exposed population within these regions, which host some of the world's megacities and major crop belts (Das et al., 2022; Zhao et al., 2022). In contrast, Mainland Southeast Asia is expected to exhibit low propagation and persistence of droughts in future timeframes (Fig. 10b), supported by increases in precipitation
360 extremes reported in previous climate change studies (Ge et al., 2021; Supharatid et al., 2022). This may contribute to its annual spatial asynchrony with EAS and SAS. While the increasing precipitation in SEA highlights the need for improved infrastructure to mitigate disasters and enhance water storage, it also presents opportunities for increased agricultural productivity. Such productivity could facilitate strategic virtual water trade (the hidden flow of water in traded commodities) among neighboring countries by revising existing regional trade agreements (Chen et al., 2024), offering mutual benefits to
365 the involved nations. Thus, the finding of drought synchrony between regions has some severe consequences, while

asynchrony   provides   an   opportunity   for   mutual   benefits.
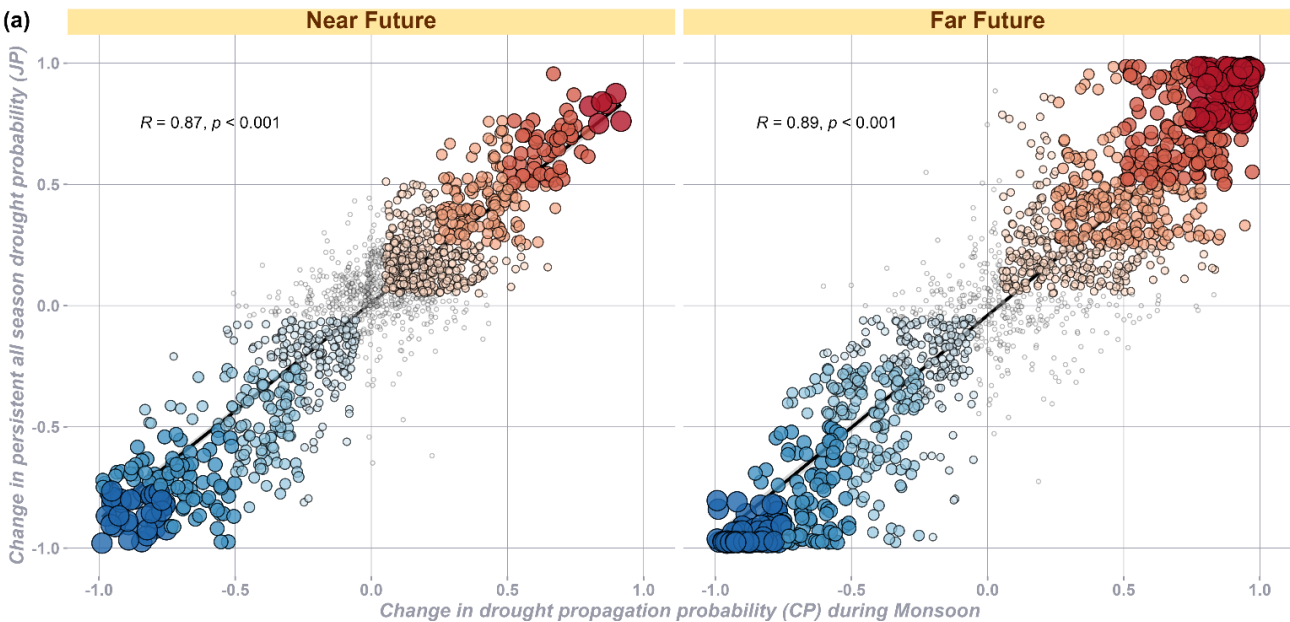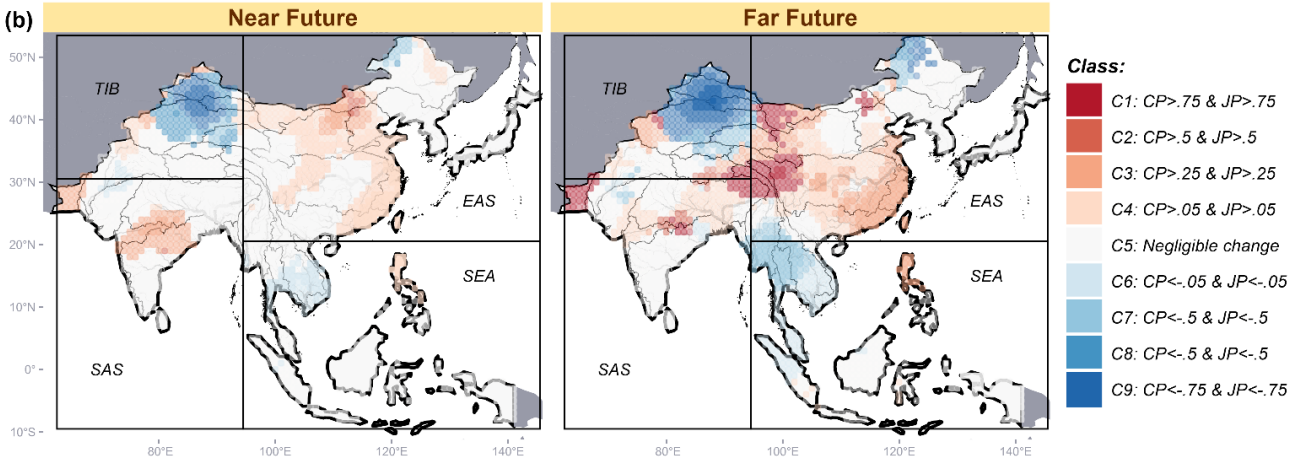

Figure 10: (a) Relationship between drought propagation and persistence using changes in their probability values between future and historical timeframes, and (b) spatial maps showing bivariate classification based on future persistence and propagation values to identify vulnerable grids.

While the present study provides a comprehensive assessment of future droughts by analyzing key characteristics such as propagation, persistence, and spatial concurrence, there are a few limitations and opportunities for further improvement. The propagation duration in this study is determined using the correlation between meteorological and agricultural drought indices with a time lag. This linear approach may oversimplify the complex nature of drought propagation. Advanced techniques, such as the phase-space reconstruction method employed by Zhao et al. (2023), could be explored in future studies, despite their higher computational demands. Additionally, the study focuses on temporal propagation but could

23

be expanded to include spatial propagation assessments. Recent works (Mondal et al., 2023; Muthuvel and Sivakumar, 2024b) that apply network theory to identify spatial drought sources have shown promise in improving the key drivers of propagation. Future research could incorporate large-scale teleconnections, as Long et al. (2024) demonstrated that these can significantly

380 influence and accelerate the propagation process. Finally, as a data-driven study, the uncertainties associated with climate model projections may impact the results, even though a multi-model ensemble was used. Addressing these uncertainties through advanced bias correction techniques or alternative ensemble methods could further enhance the robustness of the findings.

5 Conclusions

385 This study investigates the impact of climate change on drought propagation from meteorological to agricultural droughts, the persistence of inter-seasonal agricultural droughts, and their spatial concurrence across monsoon-dominant Asian regions using a copula-based probabilistic approach. While future month-wise propagation durations are expected to follow the historical monsoon pattern, an accelerated propagation rate, indicated by conditional probability, is projected in South Asia (except Western and Peninsula India) and Eastern China, increasing vulnerability to frequent agricultural droughts. Random

390 forest models identify temperature rise as the primary driver of agricultural droughts, with the Tibetan Plateau experiencing increased propagation and persistent all-season agricultural droughts in the far future. Additionally, populous regions in South and East Asia may face frequent simultaneous monsoonal agricultural droughts, exacerbating water stress and crop losses, while Southeast Asia could experience reduced spatial concurrence of droughts, potentially fostering more collaborative virtual water transfer. This study enhances drought research by examining the interrelated aspects of temporal propagation,

395 persistence, and spatial concurrence, revealing a strong connection between drought propagation and persistence in future scenarios. While acknowledging limitations such as climate model uncertainty and linear assumptions in propagation duration calculations, the findings offer valuable insights for drought planning and adaptation in the context of climate change.

Code and data availability: Freely available open-access data have been used in the study and analysed using R coding
400 language and are cited appropriately in the article.

Author contributions: DM and XQ conceptualized and developed the methodological framework. DM wrote the code and drafted the manuscript. XQ revised and edited the manuscript.

405 *Competing interests:* The authors declare that they have no conflict of interest.

References

Asquith, W.H.: lmomco---L-moments, censored L-moments, trimmed L-moments, L-comoments, and many distributions. R

415 package version 2.5.1, Texas Tech University, Lubbock, Texas. https://cran.r-project.org/web/packages/rvinecopulib/index.html, 2024.

Barker, L. J., Hannaford, J., Chiverton, A., and Svensson, C.: From meteorological to hydrological drought using standardised indicators, Hydrol Earth Syst Sci, 20, 2483–2505, https://doi.org/10.5194/hess-20-2483-2016, 2016.

Bevacqua, A. G., Chaffe, P. L. B., Chagas, V. B. P., and AghaKouchak, A.: Spatial and temporal patterns of propagation from

420 meteorological to hydrological droughts in Brazil, J Hydrol (Amst), 603, https://doi.org/10.1016/j.jhydrol.2021.126902, 2021.

Breiman, L.: Random Forests, 5–32 pp., 2001.

Chen, R., Adu, D. T., Li, W., and Wilson, N. L. W.: Virtual water trade: Does bilateral tariff matter?, Ecological Economics, 222, https://doi.org/10.1016/j.ecolecon.2024.108216, 2024.

Chen, Y. D., Zhang, Q., Xiao, M., Singh, V. P., and Zhang, S.: Probabilistic forecasting of seasonal droughts in the Pearl River

425 basin, China, Stochastic Environmental Research and Risk Assessment, 30, 2031–2040, https://doi.org/10.1007/s00477-015-1174-6, 2016.

Dai, M., Huang, S., Huang, Q., Zheng, X., Su, X., Leng, G., Li, Z., Guo, Y., Fang, W., and Liu, Y.: Propagation characteristics and mechanism from meteorological to agricultural drought in various seasons, J Hydrol (Amst), 610, https://doi.org/10.1016/j.jhydrol.2022.127897, 2022.

430 Das, J., Manikanta, V., and Umamahesh, N. V.: Population exposure to compound extreme events in India under different emission and population scenarios, Science of the Total Environment, 806, https://doi.org/10.1016/j.scitotenv.2021.150424, 2022.

Datta, R. and Reddy, M. J.: Trivariate frequency analysis of droughts using copulas under future climate change over Vidarbha region in India, Stochastic Environmental Research and Risk Assessment, 37, 3855–3877, https://doi.org/10.1007/s00477-

435 023-02484-3, 2023.

Fang, W., Huang, S., Huang, G., Huang, Q., Wang, H., Wang, L., Zhang, Y., Li, P., and Ma, L.: Copulas-based risk analysis for inter-seasonal combinations of wet and dry conditions under a changing climate, International Journal of Climatology, 39, 2005–2021, https://doi.org/10.1002/joc.5929, 2019.

Feng, S., Gu, X., Guan, Y., Wang, Q. J., Wang, L., Du, L., He, J., Zhang, X., and Kong, D.: Anthropogenic exacerbations of
440   summer-autumn compound dry-hot severity in the middle and lower reaches of the Yangtze River, J Hydrol (Amst), 646,
https://doi.org/10.1016/j.jhydrol.2024.132346, 2025.

Ford, T. and Labosier, C. F.: Spatial patterns of drought persistence in the Southeastern United States, International Journal of
Climatology, 34, 2229–2240, https://doi.org/10.1002/joc.3833, 2014.

Gaupp, F., Pflug, G., Hochrainer-Stigler, S., Hall, J., and Dadson, S.: Dependency of Crop Production between Global
445   Breadbaskets: A Copula Approach for the Assessment of Global and Regional Risk Pools, Risk Analysis, 37, 2212–2228,
https://doi.org/10.1111/risa.12761, 2017.

Gaupp, F., Hall, J., Hochrainer-Stigler, S., and Dadson, S.: Changing risks of simultaneous global breadbasket failure,
https://doi.org/10.1038/s41558-019-0600-z, 1 January 2020.

Ge, F., Zhu, S., Luo, H., Zhi, X., and Wang, H.: Future changes in precipitation extremes over Southeast Asia: Insights from
450   CMIP6 multi-model ensemble, Environmental Research Letters, 16, https://doi.org/10.1088/1748-9326/abd7ad, 2021.

Guo, D., Westra, S., and Maier, H. R.: Sensitivity of potential evapotranspiration to changes in climate variables for different
Australian climatic zones, Hydrol Earth Syst Sci, 21, 2107–2126, https://doi.org/10.5194/hess-21-2107-2017, 2017.

Guo, Y., Huang, S., Huang, Q., Leng, G., Fang, W., Wang, L., and Wang, H.: Propagation thresholds of meteorological drought
for triggering hydrological drought at various levels, Science of the Total Environment, 712,
455   https://doi.org/10.1016/j.scitotenv.2020.136502, 2020.

Han, Z., Huang, S., Huang, Q., Leng, G., Wang, H., Bai, Q., Zhao, J., Ma, L., Wang, L., and Du, M.: Propagation dynamics
from meteorological to groundwater drought and their possible influence factors, J Hydrol (Amst), 578,
https://doi.org/10.1016/j.jhydrol.2019.124102, 2019.

Hao, Z. and AghaKouchak, A.: Multivariate Standardized Drought Index: A parametric multi-index model, Adv Water Resour,
460   57, 12–18, https://doi.org/10.1016/j.advwatres.2013.03.009, 2013.

Hao, Z., Hao, F., Singh, V. P., Sun, A. Y., and Xia, Y.: Probabilistic prediction of hydrologic drought using a conditional
probability approach based on the meta-Gaussian model, J Hydrol (Amst), 542, 772–780,
https://doi.org/10.1016/j.jhydrol.2016.09.048, 2016.

Leng, X., Feng, X., Fu, B., Shi, Q., Ye, H., and Zhang, Y.: 'Asian water towers' are not a sustainable solution to the downstream
465   water crisis, Science of the Total Environment, 856, https://doi.org/10.1016/j.scitotenv.2022.159237, 2023.

Li, X., Long, D., Scanlon, B. R., Mann, M. E., Li, X., Tian, F., Sun, Z., and Wang, G.: Climate change threatens terrestrial
water storage over the Tibetan Plateau, Nat Clim Chang, 12, 801–807, https://doi.org/10.1038/s41558-022-01443-0, 2022.

Li, Y., Huang, S., Wang, H., Huang, Q., Li, P., Zheng, X., Wang, Z., Jiang, S., Leng, G., Li, J., and Peng, J.: Warming and
greening exacerbate the propagation risk from meteorological to soil moisture drought, J Hydrol (Amst), 622,
470   https://doi.org/10.1016/j.jhydrol.2023.129716, 2023.

Liang, J., Meng, C., Wang, J., Pan, X., and Pan, Z.: Projections of mean and extreme precipitation over China and their resolution dependence in the HighResMIP experiments, Atmos Res, 293, https://doi.org/10.1016/j.atmosres.2023.106932, 2023.

Long, J., Xu, C., Wang, Y., and Zhang, J.: From meteorological to agricultural drought: Propagation time and influencing
475   factors over diverse underlying surfaces based on CNN-LSTM model, Ecol Inform, 82, https://doi.org/10.1016/j.ecoinf.2024.102681, 2024.

Lv, B., Hao, Z., Ma, Q., Chen, Y., Zhang, X., Fu, Y., and Hao, F.: Spatial compounding of droughts and hot extremes across southwest and east China resulting from energy linkages, J Hydrol (Amst), 631, https://doi.org/10.1016/j.jhydrol.2024.130827, 2024.

480   Lv, B., Hao, Z., Jiang, Y., Ma, Q., and Zhang, Y.: Large ensemble simulations indicate increases in spatial compounding of droughts and hot extremes across multiple croplands in China, Glob Planet Change, 245, https://doi.org/10.1016/j.gloplacha.2024.104670, 2025.

Massicotte, P. and South, A.: _rnaturalearth: World Map Data from Natural Earth_. R package version 1.0.1, https://CRAN.R-project.org/package=rnaturalearth, 2023.

485   Mehrabi, Z. and Ramankutty, N.: Synchronized failure of global crop production, Nat Ecol Evol, 3, 780–786, https://doi.org/10.1038/s41559-019-0862-x, 2019.

Mondal, S., K. Mishra, A., Leung, R., and Cook, B.: Global droughts connected by linkages between drought hubs, Nat Commun, 14, 144, https://doi.org/10.1038/s41467-022-35531-8, 2023.

Muetzelfeldt, M. R., Schiemann, R., Turner, A. G., Klingaman, N. P., Vidale, P. L., and Roberts, M. J.: Evaluation of Asian
490   summer precipitation in different configurations of a high-resolution general circulation model in a range of decision-relevant spatial scales, Hydrol Earth Syst Sci, 25, 6381–6405, https://doi.org/10.5194/hess-25-6381-2021, 2021.

Muthuvel, D. and Mahesha, A.: Copula-Based Frequency and Coincidence Risk Analysis of Floods in Tropical-Seasonal Rivers, J Hydrol Eng, 26, 05021007, https://doi.org/10.1061/(asce)he.1943-5584.0002061, 2021.

Muthuvel, D. and Sivakumar, B.: Cascading spatial drought network: A complex networks approach to track propagation of
495   meteorological droughts to agricultural droughts, J Environ Manage, 370, 122511, https://doi.org/10.1016/j.jenvman.2024.122511, 2024a.

Muthuvel, D. and Sivakumar, B.: Spatial propagation of different drought types and their concurrent societal risks: A complex networks-based analysis, J Hydrol (Amst), 636, 131247, https://doi.org/10.1016/j.jhydrol.2024.131247, 2024b.

Muthuvel, D., Sivakumar, B., and Mahesha, A.: Future global concurrent droughts and their effects on maize yield, Science
500   of the Total Environment, 855, 158860, https://doi.org/10.1016/j.scitotenv.2022.158860, 2023.

Nagler, T. and Vatter, T.: _rvinecopulib: High Performance Algorithms for Vine Copula Modeling_. R package version 0.6.3.1.1, https://CRAN.R-project.org/package=rvinecopulib, 2023.

Van Noordwijk, M., Tanika, L., and Lusiana, B.: Flood risk reduction and flow buffering as ecosystem services - Part 2: Land use and rainfall intensity effects in Southeast Asia, Hydrol Earth Syst Sci, 21, 2341–2360, https://doi.org/10.5194/hess-21-

505   2341-2017, 2017.

Prabhakar, A., Mitra, S., and Varghese, F. C.: Multi-index characterization of compound dry hot events in India, International Journal of Climatology, 43, 6243–6267, https://doi.org/10.1002/joc.8203, 2023.

R Core Team: _R: A Language and Environment for Statistical Computing_. R Foundation for Statistical Computing, Vienna, Austria, https://www.R-project.org, 2024.

510   Raftery, A., Hoeting, J., Volinsky, C., Painter, I., and Yeung, K.: _BMA: Bayesian Model Averaging_. R package version 3.18.19, https://CRAN.R-project.org/package=BMA, 2024.

Rodell, M., Houser, P. R., Jambor, U., Gottschalck, J., Mitchell, K., Meng, C. J., Arsenault, K., Cosgrove, B., Radakovich, J., Bosilovich, M., Entin, J. K., Walker, J. P., Lohmann, D., and Toll, D.: The Global Land Data Assimilation System, Bull Am Meteorol Soc, 85, 381–394, https://doi.org/10.1175/BAMS-85-3-381, 2004.

515   Sadhwani, K. and Eldho, T. I.: Assessing the Effect of Future Climate Change on Drought Characteristics and Propagation from Meteorological to Hydrological Droughts—A Comparison of Three Indices, Water Resources Management, 38, 441–462, https://doi.org/10.1007/s11269-023-03679-7, 2024.

Sarhadi, A., Ausín, M. C., Wiper, M. P., Touma, D., and Diffenbaugh, N. S.: Multidimensional risk in a nonstationary climate: Joint probability of increasingly severe warm and dry conditions, Sci. Adv, 3487–3515 pp., 2018.

520   Shah, D. and Mishra, V.: Integrated Drought Index (IDI) for Drought Monitoring and Assessment in India, Water Resour Res, 56, 0–2, https://doi.org/10.1029/2019WR026284, 2020.

Singh, V. and Qin, X.: Study of rainfall variabilities in Southeast Asia using long-term gridded rainfall and its substantiation through global climate indices, J Hydrol (Amst), 585, https://doi.org/10.1016/j.jhydrol.2019.124320, 2020.

Supharatid, S., Aribarg, T., and Nafung, J.: Bias-corrected CMIP6 climate model projection over Southeast Asia, Theor Appl

525   Climatol, 147, 669–690, https://doi.org/10.1007/s00704-021-03844-1, 2022.

Tian, X., Di, Z., Yao, Y., Liu, Z., Meng, H., Sun, H., Wang, X., and Zhang, W.: Evaluation and simulation of terrestrial latent heat flux globally: A collaborative effort utilizing CMIP6 climate models and eddy covariance observations, Agric For Meteorol, 362, https://doi.org/10.1016/j.agrformet.2024.110371, 2025.

Tripathy, K. P., Mukherjee, S., Mishra, A. K., Mann, M. E., and Park Williams, A.: Climate change will accelerate the high-

530   end risk of compound drought and heatwave events, Proc Natl Acad Sci U S A, 120, https://doi.org/10.1073/pnas.2219825120, 2023.

Try, S. and Qin, X.: Evaluation of Future Changes in Climate Extremes over Southeast Asia Using Downscaled CMIP6 GCM Projections, Water (Switzerland), 16, https://doi.org/10.3390/w16152207, 2024.

Wang, L., Li, Y., Li, M., Li, L., Liu, F., Liu, D. L., and Pulatov, B.: Projection of precipitation extremes in China's mainland

535   based on the statistical downscaled data from 27 GCMs in CMIP6, Atmos Res, 280, https://doi.org/10.1016/j.atmosres.2022.106462, 2022.

Wang, T., Tu, X., Singh, V. P., Chen, X., Lin, K., Zhou, Z., and Tan, Y.: Assessment of future socioeconomic drought based on CMIP6: evolution, driving factors and propagation, J Hydrol (Amst), 617, https://doi.org/10.1016/j.jhydrol.2022.129009, 2023.

540   Wang, Z., Chang, J., Wang, Y., Yang, Y., Guo, Y., Yang, G., and He, B.: Temporal and spatial propagation characteristics of meteorological drought to hydrological drought and influencing factors, Atmos Res, 299, https://doi.org/10.1016/j.atmosres.2023.107212, 2024.

WCRP: World Climate Research Program. https://esgf-node.ipsl.upmc.fr/search/cmip6-ipsl (last access: 3 April 2024), 2024.

Williams, J. M.: Stagnant Rivers: Transboundary water security in South and Southeast Asia, Water (Switzerland), 10, 545   https://doi.org/10.3390/w10121819, 2018.

Wickham, H.: ggplot2: Elegant Graphics for Data Analysis. Springer-Verlag New York, https://cran.r-project.org/web/packages/ggplot2/index.html, 2016.

Wu, D. and Hu, Z.: Characterization of drought propagation over the Tibetan Plateau, J Hydrol Reg Stud, 56, https://doi.org/10.1016/j.ejrh.2024.102035, 2024.

550   Xiao, M., Zhang, Q., Singh, V. P., and Chen, X.: Probabilistic forecasting of seasonal drought behaviors in the Huai River basin, China, Theor Appl Climatol, 128, 667–677, https://doi.org/10.1007/s00704-016-1733-x, 2017.

Xu, P., Zhang, Z., Wang, D., Singh, V. P., Zhang, C., Fu, X., and Wang, L.: A time-varying Copula-based approach to quantify the effects of antecedent drought on hot extremes, J Hydrol (Amst), 627, https://doi.org/10.1016/j.jhydrol.2023.130418, 2023.

Xu, Y., Zhang, X., Hao, Z., Singh, V. P., and Hao, F.: Characterization of agricultural drought propagation over China based 555   on bivariate probabilistic quantification, J Hydrol (Amst), 598, https://doi.org/10.1016/j.jhydrol.2021.126194, 2021.

Yu, J., Zou, L., Xia, J., Dou, M., Liu, H., and Zuo, L.: Future changes in hydrological drought across the Yangtze River Basin: identification, spatial–temporal characteristics, and concurrent probability, J Hydrol (Amst), 625, https://doi.org/10.1016/j.jhydrol.2023.130057, 2023.

Zhang, H., Ding, J., Wang, Y., Zhou, D., and Zhu, Q.: Investigation about the correlation and propagation among 560   meteorological, agricultural and groundwater droughts over humid and arid/semi-arid basins in China, J Hydrol (Amst), 603, https://doi.org/10.1016/j.jhydrol.2021.127007, 2021.

Zhang, Q., Shen, Z., Pokhrel, Y., Farinotti, D., Singh, V. P., Xu, C. Y., Wu, W., and Wang, G.: Oceanic climate changes threaten the sustainability of Asia's water tower, Nature, 615, 87–93, https://doi.org/10.1038/s41586-022-05643-8, 2023.

Zhang, X., Hao, Z., Singh, V. P., Zhang, Y., Feng, S., Xu, Y., and Hao, F.: Drought propagation under global warming: 565   Characteristics, approaches, processes, and controlling factors, https://doi.org/10.1016/j.scitotenv.2022.156021, 10 September 2022.

Zhao, F., Wu, Y., Yin, X., Sun, K., Ma, S., Zhang, S., Liu, S., Wang, W., and Chen, J.: Projected changes in population exposure to drought in China under CMIP6 forcing scenarios, Atmos Environ, 282, https://doi.org/10.1016/j.atmosenv.2022.119162, 2022.

570   Zhao, Y., Zhu, T., Zhou, Z., Cai, H., and Cao, Z.: Detecting nonlinear information about drought propagation time and rate
       with nonlinear dynamic system and chaos theory, J Hydrol (Amst), 623, https://doi.org/10.1016/j.jhydrol.2023.129810, 2023.

       Zhou, M., Tian, F., Lall, U., and Hu, H.: Insights from a joint analysis of Indian and Chinese monsoon rainfall data, Hydrol
       Earth Syst Sci, 15, 2709–2715, https://doi.org/10.5194/hess-15-2709-2011, 2011.

       Zhou, Z., Shi, H., Fu, Q., Ding, Y., Li, T., Wang, Y., and Liu, S.: Characteristics of Propagation From Meteorological Drought
575   to Hydrological Drought in the Pearl River Basin, Journal of Geophysical Research: Atmospheres, 126,
       https://doi.org/10.1029/2020JD033959, 2021.

       Zhou, Z., Ding, Y., Fu, Q., Wang, C., Wang, Y., Cai, H., Liu, S., Huang, S., and Shi, H.: Insights from CMIP6 SSP scenarios
       for future characteristics of propagation from meteorological drought to hydrological drought in the Pearl River Basin, Science
       of the Total Environment, 899, https://doi.org/10.1016/j.scitotenv.2023.165618, 2023.

580   Zhou, Z., Wang, P., Li, L., Fu, Q., Ding, Y., Chen, P., Xue, P., Wang, T., and Shi, H.: Recent development on drought
       propagation: A comprehensive review, https://doi.org/10.1016/j.jhydrol.2024.132196, 1 December 2024.